Appl Phys B (2012) 106:939–944
DOI 10.1007/s00340-012-4928-6

Applied Physics B
Lasers and Optics

Adaptive optics correction based on stochastic parallel gradient descent technique under various atmospheric scintillation conditions: numerical simulation

H. Ma · C. Fan · P. Zhang · J. Zhang · C. Qiao · H. Wang

Received: 17 April 2011 / Revised version: 29 June 2011 / Published online: 2 March 2012

Abstract An adaptive optics system utilizing a Shack–Hartmann wavefront sensor and a deformable mirror can successfully correct a distorted wavefront by the conjugation principle. However, if a wave propagates over such a path that scintillation is not negligible, the appearance of branch points makes least-squares reconstruction fail to estimate the wavefront effectively. An adaptive optics technique based on the stochastic parallel gradient descent (SPGD) control algorithm is an alternative approach which does not need wavefront information but optimizes the performance metric directly. Performance was evaluated by simulating a SPGD control system and conventional adaptive correction with least-squares reconstruction in the context of a laser beam projection system. We also examined the relative performance of coping with branch points by the SPGD technique through an example. All studies were carried out under the conditions of assuming the systems have noise-free measurements and infinite time control bandwidth. Results indicate that the SPGD adaptive system always performs better than the system based on the least-squares wavefront reconstruction technique in the presence of relatively serious intensity scintillations. The reason is that the SPGD adaptive system has the ability of compensating a discontinuous phase, although the phase is not detected and reconstructed.

H. Ma · C. Fan (✉) · P. Zhang · J. Zhang · C. Qiao · H. Wang
Key Lab of Atmospheric Composition and Optical Radiation, Anhui Institute of Optics and Fine Mechanics, Chinese Academy of Sciences, P.O. Box 1125, Hefei 230031, China
e-mail: cyfan@aiofm.ac.cn
Fax: +86-551-5591514

1 Introduction

The conventional adaptive optics compensation technique based on the phase-conjugation principle has been successfully applied in many optical engineering fields [1, 2]. The adaptive optics system is composed of three main parts [3]: (i) a wavefront sensor for detecting the information of the distorted wavefront induced by turbulence; (ii) a wavefront corrector for correcting this aberration; and (iii) a wavefront controller for processing the measurements of the wavefront sensor and generating control commands for the wavefront corrector. However, conventional compensation for propagation through deep turbulence or over long distances is quite poor because intensity scintillation in the receiver aperture becomes a significant effect [4]. Theory and experimental results [5, 6] have shown that branch points occur in the received optical-field phase plane in these propagation situations, so wavefront measurements and phase reconstruction becomes quite challenging, which degrades the adaptive optical system's performance in some applications. Examples of systems whose performance is degraded by this factor include laser weapon systems and laser communication systems [7, 8]. In these cases, scintillation induced by turbulence can reduce the energy density at the target or reduce the signal-to-noise ratio. Thus, recent interest is increasing in the problem area of projecting a laser beam under conditions where scintillation is not negligible, that is to say, both phase and amplitude effects will corrupt the propagating wavefront in the receiver plane or at the target. Even though aberration caused by amplitude fluctuation is not considered, effective reconstruction of conjugated phase is not yet easy to realize with the Shack–Hartmann wavefront sensor.

The least-squares reconstruction regime is most widely used in adaptive optics systems [2, 5]. The basic principle of least-squares reconstruction is given as follows. The

phase gradient calculated from the Shack–Hartmann wavefront sensor is related to the wavefront by the following expression:

$$g = \mathbf{F}\phi, \tag{1}$$

where g is a vector of x- and y-phase gradients denoted by the wavefront ϕ to be reconstructed and $\mathbf{F}$ is a matrix which relates the phase gradients, also referred to as the geometry matrix. The least-squares estimate reconstruction wavefront ϕ_{LS} can be expressed by [5, 9]

$$\phi_{\mathrm{LS}} = \left(\mathbf{F}^{\mathrm{T}}\mathbf{F}\right)^{-1}\mathbf{F}^{\mathrm{T}}g. \tag{2}$$

Least-squares reconstructions are not sensitive to the presence of branch points, and as a result there is a component of the incident phase that conventional reconstructions cannot reconstruct, which is necessarily discontinuous [5].

The presence of branch points is necessarily associated with amplitude fluctuation or scintillation in the optical field [10]. The so-called Rytov variance σ_{R}^2 is typically used as a measure of the strength of the atmospheric scintillation, which for spherical wave propagation through turbulence is expressed as [11]

$$\sigma_{\mathrm{R}}^2 = 2.25k^{7/6}\int_0^L C_n^2(z)z^{5/6}(1 - z/L)^{5/6}\,\mathrm{d}z. \tag{3}$$

where $k = 2\pi/\lambda$ is the optical wave number, L is the propagation length between transmitter and receiver, $C_n^2(z)$ is the structure constant of the turbulence, and the integration is along the path of propagation. When $C_n^2(z)$ is constant over the path, we obtain

$$\sigma_{\mathrm{R}}^2 = 0496k^{7/6}L^{11/6}C_n^2. \tag{4}$$

The Rytov variance σ_{R}^2 represents the variance of the log-intensity fluctuations of the receiver plane arising from an initially spherical wave that passed through a region of length L characterized by turbulence of strength $C_n^2(z)$ as predicted by the Rytov approximation. Generally, weak and strong irradiance fluctuations are distinguished by the following expressions [11]:

$$\begin{aligned} &\sigma_{\mathrm{R}}^2 < 1 \quad \text{(weak fluctuation conditions)},\\ &\sigma_{\mathrm{R}}^2 \gg 1 \quad \text{(strong fluctuation conditions)}. \end{aligned} \tag{5}$$

As interest increases in using adaptive optical systems to propagate laser beams over long distances or strong turbulence paths, understanding the opportunities for improving adaptive optics systems' performance is increasingly important. Recently, an alternative adaptive optics system by using stochastic optimization algorithms [14, 15] was developed. This correction technique requires defining a system performance metric that is optimized by the algorithm directly. Superiorly, this adaptive optics correction system without wavefront sensor involves simple components and low cost. In addition, the selection of an appropriate and effective algorithm is significant. So far, many research results indicate that the stochastic parallel gradient descent (SPGD) algorithm is the most efficient optimization algorithm in some aspects [16], such as convergence rate, instability, the selection of control parameters and the probability of falling into local extremes. As regards the developing of the adaptive optical technique and the extending of its application field, adaptive optical correction for laser propagation over long distances is becoming quite meaningful.

In this paper we establish an adaptive optics correction system simulation model based on SPGD for a laser beam projecting system. An adaptive optics reference beam is provided as a point source located at the target. In order to find whether the correction technique based on the SPGD algorithm is more efficient than the conventional correction technique with least-squares reconstruction in the situation of intensity scintillation, even the wavefront sensor with ideal spatial resolution, we compare the two correction techniques in the same atmospheric turbulence scenario. We also examine whether the SPGD technique has the compensation ability for a discontinuous phase, and a simulation example of compensating a discontinuous phase is also presented. Specifically, the noise-free measurement and infinite temporal resolution are assumed for both simulation systems.

The following sections of this paper are organized as follows. The relevant theory of SPGD mathematical models and algorithm is presented in Sect. 2. The simulation conditions are described and results of the numerical simulations performed are analyzed in Sect. 3. Conclusions are drawn in Sect. 4.

2 Description of SPGD control model

In an adaptive optics correction system, the distorted phase $\varphi(\boldsymbol{r})$ is compensated by the phase ψ_{c} introduced by wavefront correctors, so the residual phase is considered as

$$\phi(\boldsymbol{r}) = \varphi(\boldsymbol{r}) + \psi_{\mathrm{c}}(\boldsymbol{r}), \tag{6}$$

where $\boldsymbol{r} = (x, y)$ is a vector in the plane orthogonal to the optical axis. Practically, the wavefront correction is realized by a high-speed tip-tilt mirror and a deformable mirror. Correspondingly, the corrected wavefront phase of the main laser beam results in the following expression:

$$\psi_{\mathrm{c}} = \psi_{\mathrm{tm}} + \psi_{\mathrm{dm}}, \tag{7}$$

where ψ_{tm} and ψ_{dm} respectively represent the phases introduced by the tip-tilt mirror and the deformable mirror. Considering the simulation system correcting the tip-tilt aberration, the phase introduced by the tip-tilt mirror is a function

of the slope of the mirror's surface and is simply expressed in Cartesian coordinates as [17]

$$\psi_{\mathrm{tm}} = u_x x + u_y y. \tag{8}$$

The variables x and y represent the phase components in the x- and y-directions, while the tip and tilt components u_x and u_y are variables determining the slope of the mirror. Changes in the tip and tilt components lead to a movement of the centroid of the image. The simulation system generates a small random perturbation $\delta u = \{\delta u_x, \delta u_y\}$ applied to x- and y-direction control of the tip-tilt mirror simultaneously.

To simplify analysis of the complete adaptic optics system, one normally considers each actuator to be independent, so the linear sum of the influence function $S_j(x, y)$ would represent the mirror surface $\psi_{\mathrm{dm}}(x, y)$. The phase introduced by the deformable mirror is [3]

$$\psi_{\mathrm{dm}}(x, y) = \sum_{j=1}^{N} V_j S_j(x, y), \tag{9}$$

where V_j represents the jth actuator amplitude and N is the actuator number of the deformable mirror. Since the results of experiment [3] show that a Gaussian represents a deformable mirror influence function quite well, the expression of the influence function $S_j(x, y)$ is described as (10):

$$S_j(x, y) = \exp\left\{\ln p \frac{(x - x_j)^2 + (y - y_j)^2}{r_{\mathrm{d}}^2}\right\}, \tag{10}$$

where (x_j, y_j) denotes the location coordinates of the jth actuator, p represents the coupling factor between the adjacent actuators, and r_{d} is the distance between the adjacent actuators.

The general optical schematic of the SPGD compensation system is shown in Fig. 1. This system is composed of a camera, an image quality analyzer that can calculate a performance metric J, a SPGD algorithm control block, and a wavefront corrector. For the SPGD correction block, it is assumed that the optimized system performance metric J is a function depending on the residual phase $\phi(\boldsymbol{r})$, that is to say $J = J[\phi(\boldsymbol{r})]$, so J will approach the extreme value when the aberration is completely removed ($\phi(\boldsymbol{r}) = 0$). Further, it is considered that an objective function J depends on a set of N parameters, $J = J[u_1, u_2, \ldots, u_N]$. The stochastic parallel perturbation technique requires a small random perturbation $\delta u^{(n)} = \{\delta u_1, \delta u_2, \ldots, \delta u_j, \ldots, \delta u_N\}^{(n)}$. The perturbation δu_j is a random number which has fixed amplitude $|\delta u_j| = \sigma$ and equal probabilities for $\delta u_j = \sigma$ and $\delta u_j = -\sigma$ [18, 19]. The performance metric change δJ caused by the control perturbation δu_j can be measured. $\delta J^{(n)} \delta u^{(n)}$ is used as the gradient estimate components, so the gradient descent iteration formula can be written as [15]

$$u^{(n+1)} = u^{(n)} + \gamma \delta J^{(n)} \delta u^{(n)}, \tag{11}$$

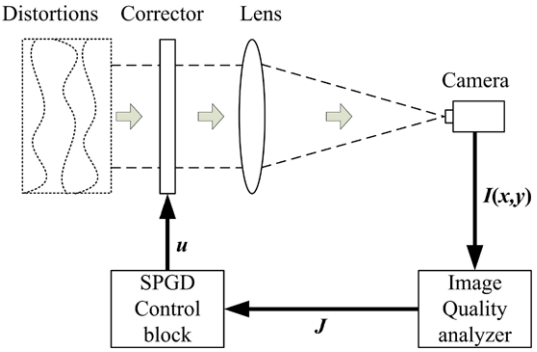

Fig. 1 Schematic of SPGD correction system

where n is the iteration number and γ is a gain coefficient. In the application, $\delta J^{(n)}$ is achieved by measurement and calculated as follows:

$$\delta J^{(n)} = J\left(u^{(n)} + \delta u^{(n)}\right) - J\left(u^{(n)} - \delta u^{(n)}\right). \tag{12}$$

The tip-tilt mirror and deformable mirror are controlled by SPGD respectively through optimizing the system performance metrics J_1 and J_2. We define J_1 as the distance between the points (x_0, y_0) and $(x_{\mathrm{c}}, y_{\mathrm{c}})$,

$$J_1 = \sqrt{(x_0 - x_{\mathrm{c}})^2 + (y_0 - y_{\mathrm{c}})^2}, \tag{13}$$

where $(x_{\mathrm{c}}, y_{\mathrm{c}})$ and (x_0, y_0) are respectively the centroid of the image while the laser travels in vacuum and in atmosphere. J_2 is considered as the mean radius, and the calculation formula is as follows:

$$J_2 = \frac{\iint_D \sqrt{(x - x_0)^2 + (y - y_0)^2} I(x, y)\, \mathrm{d}x\, \mathrm{d}y}{\iint_D I(x, y)\, \mathrm{d}x\, \mathrm{d}y}, \tag{14}$$

where D is the area occupied by the laser intensity distribution, (x_0, y_0) are the centroid coordinates of the image, and $I(x, y)$ is the far-field light intensity in position (x, y).

3 Numerical results and analysis

3.1 Simulation description

The schematic of the simulation projection system follows the basic concept as shown in Fig. 3. An adaptive optics reference beam is provided as a point-source beacon located at the target. The outgoing laser beam was focused with a transmitting telescope to where the target was located. The main parameters used in the simulation are presented in Table 1. We modeled propagation of the laser beam through turbulence as a sequence of two-dimensional wave propagations from one thin phase screen to another using scalar diffraction theory [12]. The fields propagating between the phase screens were calculated by a sequence of numerically

efficient fast-Fourier-transform (FFT) operations. The random phase screens were generated with von Karman spectrum distributions by white-noise filtering in the Fourier domain [20]. Forty independent statistical turbulence-induced phase screens were laid over the propagation path. A non-adaptive transformation [13] was adopted in the propagation calculation, so the speed and the accuracy of computation are ensured. Besides, it is assumed that the propagation path is near horizontal and the turbulence distribution is uniform.

A 61-element deformable mirror was utilized in the simulation. The deformable mirror configurations are shown in Fig. 2. The value of the coupling factor p and the distance between the adjacent actuators r_d are given in Table 1. In the simulation, we fix the ratio $D/r_0 = 7$ and adjust the Rytov variance by changing the strength of the turbulence and the propagation length. Knowing that a mechanically deformable mirror surface cannot exactly match the aberration patterns of the eddies of atmospheric turbulence, Hudgin developed an expression of the fitting error to show the wavefront error that resulted after a least-squares fit between the surface and the atmosphere [3],

$$\sigma_{\text{fit}}^2 = \kappa (r_d/r_0)^{5/3}, \tag{15}$$

where the parameter κ is set to 0.23 for Gaussian influence.

The performance of an adaptive optics system is usually characterized by the Strehl ratio. Results of a long-exposure average help to reveal the statistical average effects of spot position wandering and spreading on the overall energy spread. The Strehl ratio is defined as the ratio of the axis intensity of a long-exposure image after propagation through turbulence and through a vacuum. The long-exposure results were averaged over an ensemble of 60 statistically independent random realizations.

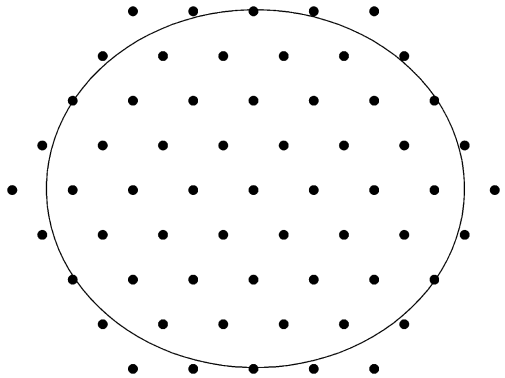

Fig. 2 Location of 61-element deformable mirror

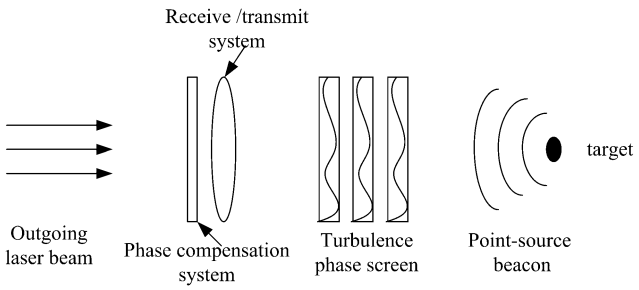

Fig. 3 Schematic of laser projection system

3.2 Simulation results

The study of the obtained character in various scintillation conditions is important for understanding the SPGD compensation system's challenges and performance. The results presented provide the very first direct comparison of these two wavefront control approaches in various atmospheric scintillation conditions with the main emphasis on compensation of volume turbulence effects. We implement the simulation as Sect. 3.1 described. There are three obtained Strehl ratio results in Fig. 4: curve (a) represents ideal phase compensation results considering the fitting error given in (15) of a 61-element deformable mirror. They are obtained by

Table 1 Parameters used in the simulation

Parameter	Value
Receive or transmit aperture diameter, D	60 cm
Wavelength, $\lambda_{\text{main}} = \lambda_{\text{beacon}}$	1.315 μm
Propagation length, L	2 km to 50 km
Turbulence structure constant, C_n^2	1.78×10^{-14} m$^{-2/3}$ to 3.55×10^{-16} m$^{-2/3}$
Fried parameter, r_0	8.57 cm
Grid number, N_g	256×256
Grid sampling interval, Δx	1 cm
Number of phase screen, N_{ps}	40
Number of turbulence realizations, N_{tr}	60
Number of deformable mirror actuators, N	61
Distance of adjacent actuators r_d	7.5 cm
Actuators' coupling factor p	15%

multiplying a factor of $\exp(-\sigma_{\text{fit}}^2)$ and the compensation results of the perfect conjugate phase calculated directly from the distortion. Curve (b) describes the results of SPGD compensation with 500 iteration steps for each frame turbulence realization. The Strehl ratio of the conventional compensation with ideal wavefront detecting is shown with curve (c). We can see that the efficiency of the ideal phase correction is not as insensitive to the value of the intensity scintillation. As the strength of the scintillation increases, the performances of both approaches are degraded, but SPGD always performs better than the conventional technique.

Figure 5 presents the number of branch-point pairs that were found in the receiver plane to which a beacon wave from a point source located at the target propagates as a function of σ_{R}^2 for the same turbulence realizations as in Fig. 4. Comparing Fig. 4 and Fig. 5, it indicates that the results of both the SPGD correction and the conventional correction are very dependent on the number of branch points.

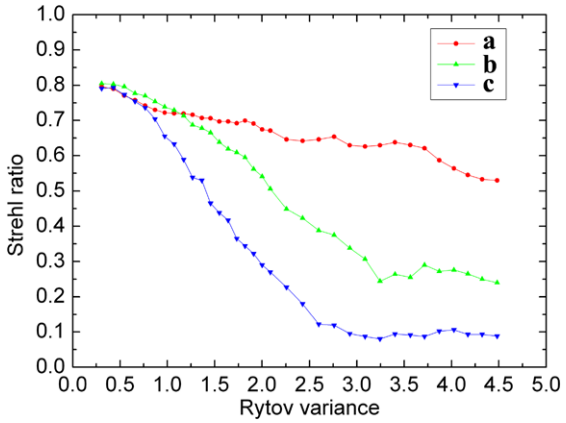

Fig. 4 Strehl ratio results versus Rytov variance: (**a**) ideal phase compensation considering 61-element deformable fitting error, (**b**) SPGD compensation with driven 61-element deformable mirror, (**c**) conventional compensation with ideal wavefront detecting and least-squares reconstruction and 61-element deformable mirror

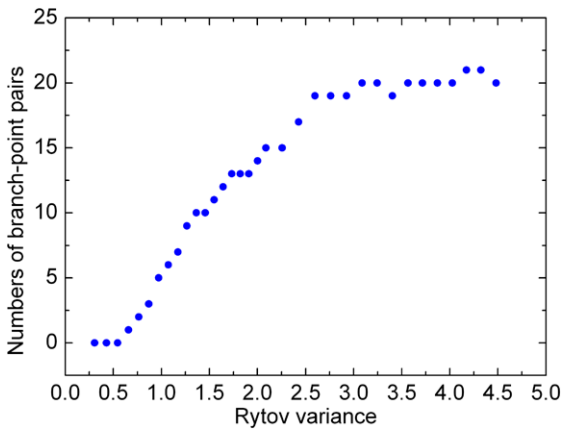

Fig. 5 Number of branch-point pairs versus Rytov variance for the same turbulence realizations as in Fig. 4

When there are few branch points, both correction curves (b) and (c) show a good agreement with curve (a). For values of σ_{R}^2 above approximately 1.0, the number of branch points is increasing lineally, and both correction results are degrading. Until the value of σ_{R}^2 reaches 3.0, the number of branch points does not increase yet, and simultaneously both correction results nearly tend to invariableness.

Accordingly, there is no phase information detected for branch points when the SPGD adaptive system works, so it is necessary to know whether the SPGD system can effectively cope with branch points in order to understand the reason for the improvement of the performance with the SPGD technique. In Fig. 6, we present an example of compensation of a discontinuous phase by SPGD and by the least-squares technique. The optical field with the complex light amplitude is given by

$$U(x, y) = (x + \mathrm{i}y)\exp\left(-x^2 - y^2\right), \tag{16}$$

where (x, y) represents the spatial location in some plane. The original phase is calculated by $\psi(x, y) = \tan^{-1}(\mathrm{Im}[U(x, y)]/\mathrm{Re}[U(x, y)])$, where $\mathrm{Re}[U(x, y)]$ and $\mathrm{Im}[U(x, y)]$ represent the real and imaginary parts of the complex field. As Fig. 6a shows, the original phase is a discontinuity, and there is a branch point in the centre. The fitting phase by the 61-element deformable mirror of the ideal conjugated phase $\psi^*(x, y)$ is given in Fig. 6b. Figure 6c shows the compensation phase, which is the surface of the deformable mirror driven by the SPGD algorithm after 500 iterations. Figure 6d shows that the reconstructed phase by the least-squares estimation that obviously performs very poorly compared with the initial phase. From the figures, we find that the SPGD compensation technique works much more perfectly with this example than least-squares reconstruction. From the figures, we can indicate that the SPGD technique can compensate a discontinuous phase without a detection and reconstruction process.

4 Conclusions

We have implemented a SPGD adaptive compensation numerical experiment for a laser beam projection system in different scintillation conditions induced by laser propagation over a near-horizontal atmospheric path in which the propagation distance is long or the turbulence is deep. The performance of the SPGD correction system has been studied by comparing that with a conventional adaptive system which is utilizing an ideal-detecting Shack–Hartmann wavefront sensor. We have also examined the ability of compensating a discontinuous phase by the SPGD control algorithm through an example comparing that with the least-squares reconstruction technique. Numerical results demonstrated that the SPGD adaptive optics technique was more efficient

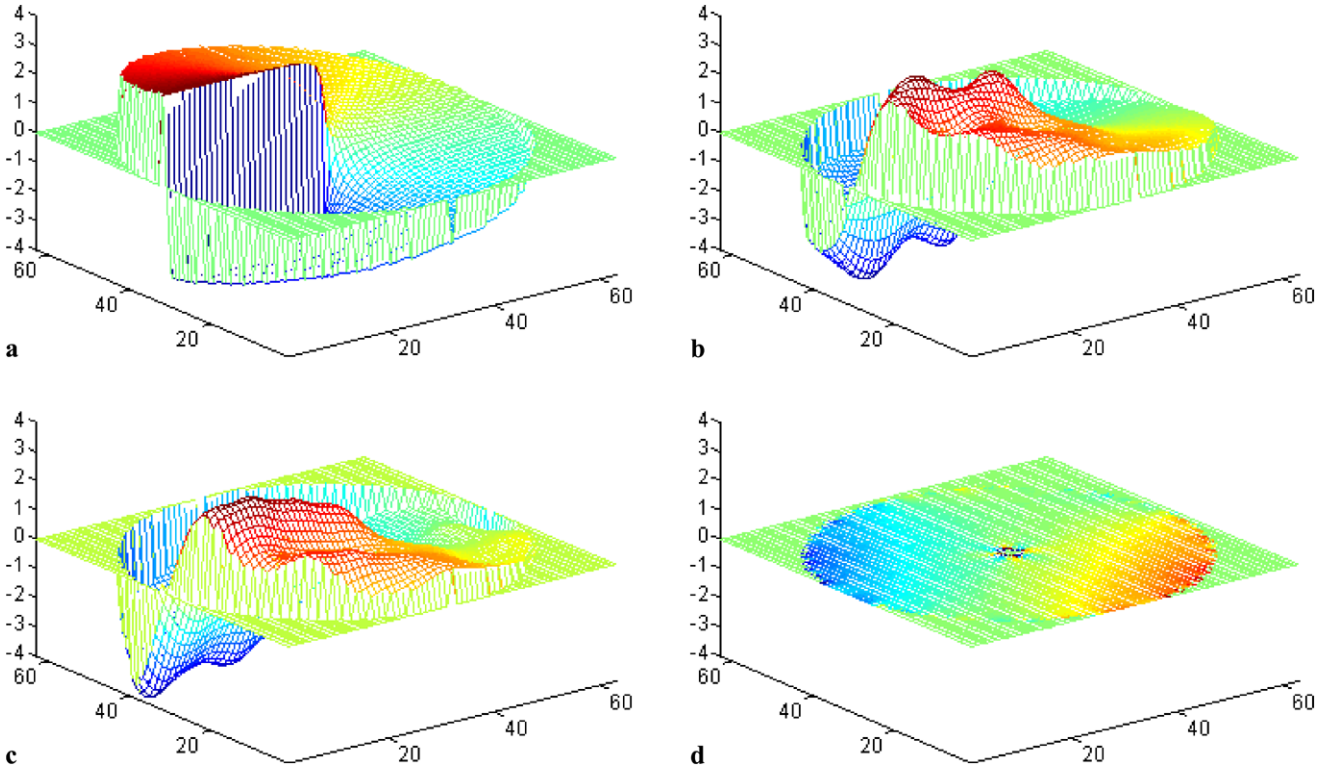

Fig. 6 (**a**) Original phase, (**b**) fitting phase by 61-element deformable mirror for ideal conjugate phase of original phase, (**c**) compensation phase by SPGD technique, (**d**) reconstruction phase by the least-squares algorithm

than the conventional adaptive optics technique in the presence of relatively serious intensity scintillations. That is because the discontinuous phase could be compensated by a deformable mirror driven by the SPGD control block, although there is no wavefront detection or special reconstruction algorithm for branch phase. Specifically, measurement noise, effects of finite spatial resolution of the deformable mirror, anisoplanatic effects, effects of time delays between wavefront sensing and correction, and SPGD iteration time delays are not addressed here. However, the results presented here may motivate future further studies of these matters.

Acknowledgements Acknowledgements This work was supported by the National High Technology Development Program of China (Grant Nos. A825021 and A825011) and the Computational Center of the Hefei Institute of Physical Science, Chinese Academy of Sciences (Grant No. 0330405002-7).

References

1. F. Roddier, *Adaptive Optics in Astronomy* (Cambridge University Press, Cambridge, 1999)
2. M.C. Roggemann, B.M. Welsh, *Imaging Through Turbulence* (CRC, Boca Raton, 1996)
3. R.K. Tyson, *Principles of Adaptive Optics* (Academic Press, San Diego, 1991)
4. N.B. Baranova, A.V. Mamaev, N.F. Pilipetsky, V.V. Shkunov, B.Y. Zel'dovich, J. Opt. Soc. Am. A **73**, 525 (1983)
5. D.L. Fried, J. Opt. Soc. Am. A **15**, 2759 (1998)
6. C.A. Primmerman, T.R. Price, R.A. Humphreys, B.G. Zollars, H.T. Brarclay, J. Herrmann, Appl. Opt. **34**, 2081 (1995)
7. M.C. Roggemann, A.C. Koivunen, J. Opt. Soc. Am. A **17**, 53 (2000)
8. R.K. Tyson, J. Opt. Soc. Am. A **19**, 753 (2002)
9. D.L. Fried, J. Opt. Soc. Am. A **67**, 370 (1976)
10. L.C. Andrews, R.L. Phillips, C.Y. Hopen, M.A. Al-Habash, J. Opt. Soc. Am. A **16**, 1417 (1999)
11. L.C. Andrews, R.L. Phillips, *Laser Beam Propagation Through Random Media* (SPIE Press, Bellingham, 2005)
12. V.P. Lukin, *Adaptive Beaming and Imaging in the Turbulent Atmosphere* (SPIE Press, Bellingham, 2002)
13. J.W. Strohbehn, *Laser Beam Propagation in the Atmosphere* (Springer, Berlin, 1978)
14. M.A. Vorontsov, G.W. Carhart, Opt. Lett. **22**, 907 (1997)
15. M.A. Vorontsov, G.W. Carhart, J. Opt. Soc. Am. A **17**, 1440 (2000)
16. H.Z. Yang, X.Y. Li, Opt. Laser Technol. **43**, 630 (2011)
17. M.S. Zakynthinaki, Y.G. Saridakis, Comput. Phys. Commun. **150**, 274 (2003)
18. J.C. Spall, IEEE Trans. Autom. Control **37**, 332 (1992)
19. J.C. Spall, *Introduction to Stochastic Search and Optimization* (Wiley, Hoboken, 2003)
20. J.M. Martin, S.M. Flatte, Appl. Opt. **27**, 2111 (1988)